

# Inspired gas-induced vascular change in tumors with magnetic-resonance-guided near-infrared imaging: human breast pilot study

**Colin M. Carpenter**<sup>\*,†</sup>

Dartmouth College  
Thayer School of Engineering  
Hanover, New Hampshire 03755

**Rebecca Rakow-Penner**

Stanford University  
School of Medicine  
Department of Radiology  
Stanford, California 94305

**Shudong Jiang**

Dartmouth College  
Thayer School of Engineering  
Hanover, New Hampshire 03755

**Bruce L. Daniel**

Stanford University  
School of Medicine  
Department of Radiology  
Stanford, California 94305

**Brian W. Pogue**

Dartmouth College  
Thayer School of Engineering  
Hanover, New Hampshire 03755

**Gary H. Glover**

Stanford University  
School of Medicine  
Department of Radiology  
Stanford, California 94305

**Keith D. Paulsen**

Dartmouth College  
Thayer School of Engineering  
Hanover, New Hampshire 03755

## 1 Introduction

Magnetic resonance-guided near infrared (MRg-NIR) imaging leverages knowledge of the location of a suspect lesion (provided by MR) to provide hemodynamic information such as total hemoglobin and oxygenation.<sup>1</sup> This study reports on the potential of contrast derived from measuring the vascular compliancy between normal and diseased tissue, which may have promising utility in increasing specificity.

<sup>\*</sup>Current affiliation: Department of Radiation Oncology, School of Medicine, Stanford University, Stanford, CA.

<sup>†</sup>Address all correspondence to: Colin M. Carpenter, Stanford University, School of Medicine, Department of Radiology, Stanford, CA 94305. Tel: (650) 725-2508; Fax: (650) 498-4015; E-mail: colincarpenter@stanford.edu.

**Abstract.** This study investigates differences in the response of breast tumor tissue versus healthy fibroglandular tissue to inspired gases. Cycles of carbogen and oxygen gas are administered while measuring the changes with magnetic-resonance-guided near-infrared imaging in a pilot study of breast cancers. For two patients, analyses are performed with cross-correlation techniques, which measure the strength of hemodynamic modulation. The results show that the overall vaso-response, indicated by total hemoglobin, of healthy tissue has approximately a 72% and 41% greater correlation to the gas stimulus than the tumor region, in two patients respectively, when background physiological changes are controlled. These data support the hypothesis that tumor vasculature has a poorly functioning vasodilatory mechanism, most likely caused by dysfunctional smooth muscle cells lining the vasculature. This study presents a methodology to quantitatively analyze inspired gas changes in human breast tumors, and demonstrates this technique in a pilot patient population.

© 2010 Society of Photo-Optical Instrumentation Engineers. [DOI: 10.1117/1.3430729]

**Keywords:** breast tumor; inspired gas change; magnetic resonance; near-infrared imaging.

Paper 09479LRR received Nov. 1, 2009; revised manuscript received Mar. 24, 2010; accepted for publication Apr. 21, 2010; published online May 26, 2010.

Tumor vasculature is known to lack proper vasomotor function because of the deficiency in smooth muscle cells lining the endothelial cells.<sup>2</sup> Thus, tumors are expected to respond differently to changes in the local environment than in normal tissue. Additionally, this contrast may also have the potential to identify tissues that are less susceptible to therapy due to their poor vascular response to changes in oxygenation.<sup>3</sup> These changes may be induced by modulated gas breathing of oxygen (Ox) and/or carbogen (Cb).<sup>4</sup> These gases are known to have opposing effects on vascular tone; whereas carbogen, containing CO<sub>2</sub>, acts as a vasodilator, oxy-

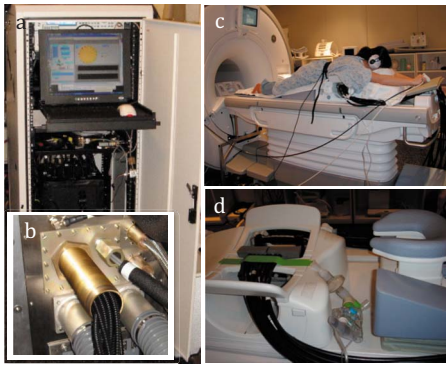


**Fig. 1** (a) The optical imaging instrument operated within the MR equipment room. (b) Optical fibers entered the MR room through a conduit in the wall, and (c) and (d) coupled to a custom interface within the MR breast coil. The respiratory apparatus is shown in (d).

gen, lacking  $\text{CO}_2$ , acts as a vasoconstrictor.<sup>5</sup> Thus, switching between these gases might intuitively induce changes in vascular tone. By determining the magnitude of vascular changes due to a respiratory stimulus, potential subjects who respond more successfully to therapy might be identified. This work presents preliminary results for a technique in characterizing breast tumors by measuring the impaired vasomotor function in tumor vasculature with MR-guided NIR imaging.

## 2 Methods

### 2.1 Magnetic Resonance-Guided Near-Infrared Imaging

NIR tomography produces quantitative images of oxyhemoglobin, deoxyhemoglobin, water content, and lipid content by sampling the absorption near-infrared light. These absorption properties are spectrally fit using known tissue absorption spectra to determine the tissue contents. This technique has been successfully applied to a number of tissues, most notably the breast and brain.

In this study, an optical imaging instrument collected data within a breast coil in a 3T MRI (Discovery MR750, GE Medical Systems, Waukesha, Wisconsin). The optical instrument, shown in Fig. 1(a), used three wavelengths (661, 785, and 826 nm) of light that were intensity modulated at unique frequencies and jointly coupled to a source illumination fiber. 16 13-m optical fibers entered the magnet room through a conduit, shown in Fig. 1(b). Light was sequentially transmitted to 16 locations around the breast and detected by 15 photomultiplier tubes acquiring data in parallel, to sample breast optical properties every 30 s. The 3T anatomical (Dixon) MR images were used to separate the fibroglandular from the adipose tissue. Tumors were identified by contrast-enhanced MRI (CE-MRI) and segmented with the aid of the radiologist (Daniel). These structural boundaries were input into an MR-coupled reconstruction algorithm to recover hemodynamic parameters for these tissues.<sup>1</sup>

### 2.2 Human Respiratory Breathing Experiments

Hemodynamics were dynamically modulated by introducing oxygen (100%  $\text{O}_2$ ) and carbogen (95% $\text{O}_2$ :5% $\text{CO}_2$ ) into the breathing circuit. Appropriate physiological monitoring equip-

ment was attached to the subjects, as shown in Fig. 1(c), and used to measure respiratory and heart rates. Subjects breathed through a mouthpiece and had their noses sealed to prevent inadvertent breathing of room air, and thus bypassing the stimulus. The oxygen and carbogen gases (Praxair, Danbury, Connecticut) were computer controlled to switch from oxygen to carbogen every two minutes for a total of four cycles, beginning with oxygen. In total, the imaging exam was 16 min (each period consisting of oxygen for 2 min and carbogen for 2 min, for four cycles). Gas from the respiratory circuit, shown in Fig. 1(d), was sampled with an oxycapnograph (Capnomac Ultima, GE Healthcare, Waukesha, Wisconsin) to monitor expired  $\text{CO}_2$ ,  $\text{O}_2$ , and respiratory rate to ensure breathing compliance. Measurements were also collected during an all air pseudo-stimulus to determine background modulation in physiology. For this air/air control stimulus, room air was breathed for 16 min. A fan inside the MR bore was operated to prevent rebreathing of the subject's exhaled air.

### 2.3 Data Analysis

Characteristics of the breast tissue response were calculated for each time point in the respiratory stimulus. Measurements of the AC amplitude and phase of the detected light intensity were calibrated by fitting measurements from the first time point to a homogeneous model for absorption and scatter. This method provides measurements that are free from fiber coupling noise. The resulting data were input into the image reconstruction along with tissue adipose, fibroglandular, and lesion boundaries to determine tissue properties in each region.

The resulting images of total hemoglobin were mean filtered in time and cross-correlated to the gas stimulus time series, which was modeled with a sinusoid with a frequency of 0.0042 Hz (corresponding to a period of 4 min). This approximation was made because respiratory physiology acts as a low-pass filter to vascular contrast.<sup>6</sup> The first period of data was dropped to account for respiratory changes due to the switch from room air to the gas stimulus.

The cross-correlation metric provided measures of correlation and time lag between the tissue response and the gas stimuli. The maximum correlation was determined by cross correlating the measured hemodynamic response with the sinusoidally modeled stimulus [the “cov” function in MATLAB (Mathworks, Natick, Massachusetts)]. The time lag at maximum correlation represents the lag in time between the gas stimulus and the response in the tissue, whereas the correlation at this time lag represents the degree to which the vasculature is affected by the gas stimulus. Correlation and time lags were calculated for healthy fibroglandular and tumor tissues.

Oxygen and carbogen breathing leads to complex changes in blood flow and hemoglobin oxygen saturation because of the interplay between  $\text{pO}_2$ ,  $\text{pCO}_2$ , and vascular function. However, we have observed that the total hemoglobin and oxygen saturation in the breast during oxygen/carbogen modulation is dominated by changes in the vasomotor function. We have also observed that some subjects do not exhibit significant changes in hemodynamics during this stimulus of gas breathing. This is probably due to the variability in metabolism, which can cause a substantial modulation of physiology independent of the respiratory stimulus.<sup>7</sup> Thus, a gas-

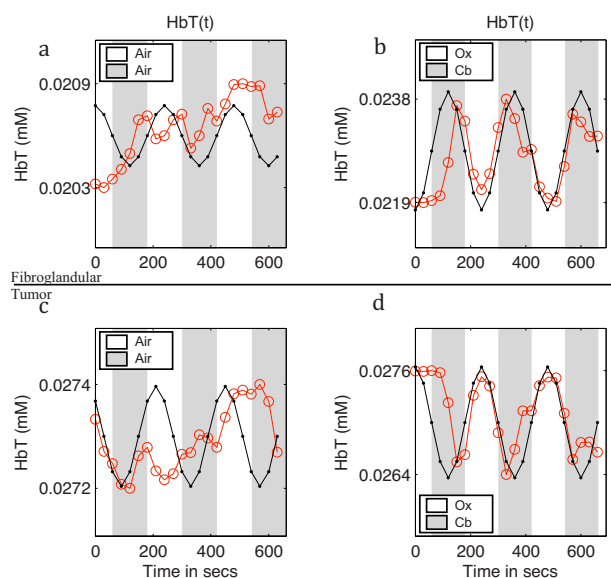


**Fig. 2** (a) and (b) Modulation of total hemoglobin in the healthy fibroglandular tissue for patient 3 (red, open circles) during (a) air/air breathing and (b) oxygen/carbogen breathing, compared to a best-fit sinusoidal (black, closed circles). In (c) and (d), a similar comparison is shown for the tumor tissue (red, open circles) during (c) air/air breathing and (d) oxygen/carbogen breathing. (Color online only.)

to-air ratio (GAR), shown in Eq. (1), is calculated as a quantitative metric to determine how large the modulation due to gas is compared to the background physiological modulation during air breathing.

$$\text{GAR} = \frac{\max(\text{corr}_{\text{gas}})}{\max(\text{corr}_{\text{air}})}. \quad (1)$$

In Eq. (1), the GAR is computed by finding the ratio of the maximum correlation of the gas to the stimulus, to the maximum correlation of the all air control.

All three subjects in this study provided informed consent, following the procedures approved by the Institutional Review Board at Stanford Medical Center. Of the three subjects, two subjects were analyzed. One subject was dropped because of lack of compliance to the breathing protocol (subject was not breathing through the mouth piece), which was apparent when examining the oxycapnometer data. Patient 2 was aged 43 years, premenopausal, and had a 1.8-cm grade-2 invasive ductal carcinoma in the left breast. Patient 3 was aged 47 years, and had a 1.2-cm grade-1 invasive ductal carcinoma of the left breast. Imaging was performed before treatment.

### 3 Results and Discussion

An example of the vascular response to the gas stimulus for both the healthy fibroglandular and tumor tissue is shown in Figs. 2(b) and 2(d), respectively. The response during an air/air control for healthy and tumor vasculature is shown in Figs. 2(a) and 2(c), respectively. MRG optical data points are plotted as open circles. Overlaid in black (with calculated points labeled as closed circles) are the best-fit sinusoids that match the data. These sinusoids are phase shifted to match the time lag of the tissue response, and normalized to the amplitude of

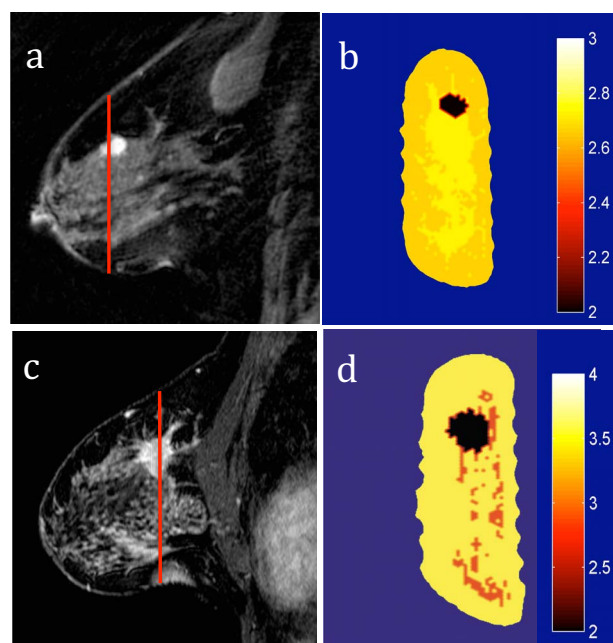


**Fig. 3** (a) CE-MR images of subject 2 and (c) subject 3 identifying breast carcinomas. The red vertical line indicates the coronal data collection plane sampled by the optical imaging system, which corresponds to the slices in (b) and (d). The GAR images of total hemoglobin for subjects 2 and 3 are shown in (b) and (d), respectively, showing lower GAR in the tumor tissue. (Color online only.)

the response. These curves allow a visual comparison of the cross correlation between the tissue response and the modeled gas stimulus. Clearly, the response during air/air breathing, shown in Figs. 2(a) and 2(c) has lesser correlation to the sinusoidal stimulus than that of oxygen/carbogen breathing, shown in Figs. 2(b) and 2(d) (0.70 versus 0.26 in healthy tissue, and 0.65 versus 0.34 in tumor tissue).

Since the vascular changes induced during gas breathing can be insignificant in some subjects, the GAR ratio was computed to compare healthy versus tumor tissue. This metric provides a means to gauge the relative magnitude of the change with respect to normal air variations caused by biological noise. The tumor regions of interest for these cases were identified by CE-MRI. These images are shown in Figs. 3(a) and 3(c). The sequences used to collect CE-MRI data were 3-D T1-weighted gradient echo images (TR/TE/flip angle=30/8/40 deg) collected on a 1.5 T MR system (Signa Excite, GE Medical Systems, Waukesha, Wisconsin). These images show regions of contrast enhancement that were histologically confirmed invasive ductal carcinomas. The optical data were collected in the plane indicated by the vertical lines in the CE-MRI images. Data from these planes were used to form images of the maximum correlation of the breast tissue to the respiratory stimulus compared to the air control.

The GAR for total hemoglobin of the tumor tissue compared to the normal surrounding fibroglandular tissue is shown in Figs. 3(b) and 3(d). There is a substantial separation in the average GAR between the normal and tumor tissue, which is on average 1.8 in tumor tissue to 2.8 on average in normal tissue, for these two patients. This GAR change is due to a weaker correlation in the tissue response to the gas stimu-

**Table 1** Cross-correlation in the fibroglandular (FG) and tumor tissue for the oxygen/carbogen (Ox/Cb) stimulus. GAR are the maximum correlations of the Ox/Cb stimulus versus the maximum correlation of the all-air control.

	Max correlation in FG, Ox/Cb	Max correlation in FG, air/air	GAR in FG	Max correlation in tumor, Ox/Cb	Max correlation in tumor, air/air	GAR in tumor
Patient 2	0.37	0.13	2.85	0.25	0.15	1.67
Patient 3	0.70	0.26	2.69	0.65	0.34	1.91

lus in these cases. These results could be explained by a lack of adequate smooth muscle cells to allow proper vasodilatory response. A similar lack of response has been observed in rodent R3230 mammary tumors by Hull et al.<sup>8</sup> where a switch from air to carbogen caused a small and variable change in total hemoglobin (possibly indicating a decreased blood flow).

These results are predicted based on histological studies in tumors that reveal inadequate smooth muscle cells lining the vasculature.<sup>2</sup> Without properly functioning smooth muscle cells to control vascular tone, blood volume changes are expected to be smaller. For example, in healthy tissue, the breathing of carbogen normally leads to vascular dilation due to the presence of CO<sub>2</sub>, a byproduct of cellular respiration. Excess CO<sub>2</sub> typically indicates that the cells are consuming more oxygen than the vasculature is transporting. The vasculature normally responds by dilating, bringing in freshly oxygenated blood. The lack of smooth muscle cells in tumor tissue prevents the vasculature from dilating, resulting in a smaller or inconsistent change to the carbogen stimulus. Conversely, the switch to oxygen gas from carbogen would lead to vascular constriction in normal tissue (in this case, due to the lack of CO<sub>2</sub>). The lack of properly functioning vasocontrol in a tumor would result in less vascular constriction. These changes are better determined with the cross-correlation metric, which provides a quantification of the agreement of the measured tissue response to the gas stimulus.

It is interesting to note that the correlation in the tumor tissue for Ox/Cb of patient 2 is less than the air/air correlation for patient 3 (see Table 1). Based on the results from a previous study,<sup>9</sup> we do not believe that comparing interpatient gas correlations has any real meaning, because there is such a large variance in air/air correlations in healthy subjects; these differences underscore the need for the GAR metric, which accounts for background physiology, and might be a way to quantitatively compare patients. As this is a pilot study, certainly a larger population needs to be measured to determine the utility of this technique.

Interestingly, the phase of the vascular change in the tumor tissue, shown in Fig. 2(d), is different than that of the healthy tissue, shown in Fig. 2(b). The phase delay (in units of  $\pi$ ) is displayed in more detail in Table 2. In both cases, there is a time lag between the healthy fibroglandular tissue response and the tumor tissue response. This indicates differences in blood delivery between the healthy and diseased tissue. This lag could be explained by a delay in the blood arriving in the tumor due to poor tissue perfusion, a well-documented characteristic of tumors.<sup>10</sup>

## 4 Conclusions

The search for increased specificity in breast cancer continues in the radiology community due to inadequate biomarkers of malignancy. Vascular functional deficiency has been noted as one of the key hallmarks of breast cancer, but tools to measure it have been inadequate. Breathing oxygenated gases has been used to investigate bladder, prostate, head and neck, and other tissues using BOLD MR imaging.<sup>11</sup> However, breast BOLD has not been well studied, presumably because of the difficulty measuring changes in hemodynamics with adequate SNR. To date, only one case has been reported of changes in a human breast tumor during hyperoxygenated gas breathing, where the mean signal change was 62%.<sup>11</sup>

Here, a pilot study is carried out using an oxygen/carbogen breathing protocol to produce hemodynamic changes. The functional changes in the tumor regions, measured by MRG optical imaging, are compared to the surrounding healthy tissue by cross correlating the measured response with the modeled breathing stimulus. This robust method provides self-referenced maps of the magnitude and time delay of vascular response of a region of interest detected during breast MR mammography.

The results show that relative total hemoglobin variation is higher in healthy tissue than tumor tissue. Additionally, the cross-correlation magnitude between the tumor tissue during inspired gas compared to an air-air control is less than that of the fibroglandular tissue compared to the control. Although this is a preliminary pilot study, this study shows the potential of using hemodynamic modulation as a tissue biomarker for diagnostic potential. Alternately, this metric could be used as a means to measure vascular function to determine sensitivity to therapy.

**Table 2** Time lag at maximum correlation between the measured total hemoglobin response and the Ox/Cb stimulus. Data are presented for the healthy surrounding fibroglandular tissue and the tumor tissue for patients 2 and 3.

	Phase delay for FG tissue (units of $\pi$ )	Phase delay for tumor tissue (units of $\pi$ )	Phase difference (units of $\pi$ )
Patient 2	1.75	1.5	0.25
Patient 3	0	1	1

### Acknowledgments

The authors acknowledge Anne Sawyer, Sandra Rodriguez, and Brian Hargreaves from the Stanford Department of Radiology. We also acknowledge funding from the Department of Defense Predoctoral Training Fellowship 503298, the National Cancer Institute grants 5P01CA080139 and 2R01CA069544, and the National Center for Research Resources Grant No. P41 RR009784.

### References

1. C. M. Carpenter, B. W. Pogue, S. J. Jiang, H. Dehghani, X. Wang, K. D. Paulsen, W. A. Wells, J. Forero, C. Kogel, J. B. Weaver, S. P. Poplack, and P. A. Kaufman, "Image-guided spectroscopy provides molecular specific information *in vivo*: MRI-guided spectroscopy of breast cancer hemoglobin, water, and scatterer size," *Opt. Lett.* **32**, 933–935 (2007).
2. A. A. Gilad, T. Israely, H. Dafni, G. Meir, B. Cohen, and M. Neeman, "Functional and molecular mapping of uncoupling between vascular permeability and loss of vascular maturation in ovarian carcinoma xenografts: the role of stroma cells in tumor angiogenesis," *Int. J. Cancer* **117**, 202–211 (2005).
3. S. Dische, M. I. Saunders, R. Sealy, I. D. Werner, N. Verma, C. Foy, and S. M. Bentzen, "Carcinoma of the cervix and the use of hyperbaric oxygen with radiotherapy: a report of a randomised controlled trial," *Radiother. Oncol.* **53**, 93–98 (1999).
4. A. Rauscher, J. Sedlacik, M. Barth, E. M. Haacke, and J. R. Reichenbach, "Noninvasive assessment of vascular architecture and function during modulated blood oxygenation using susceptibility weighted magnetic resonance imaging," *Magn. Reson. Med.* **54**, 87–95 (2005).
5. J. West, *Respiratory Physiology: The Essentials*, 8th ed., Lippincott, Williams and Wilkins, Philadelphia, PA (2008).
6. R. B. King, A. Deussen, G. M. Raymond, and J. B. Bassingthwaite, "A vascular transport operator," *Am. J. Physiol.* **265**, H2196–208 (1993).
7. M. J. Brischetto, R. P. Millman, D. D. Peterson, D. A. Silage, and A. I. Pack, "Effect of aging on ventilatory response to exercise and CO<sub>2</sub>," *J. Appl. Physiol.: Respir., Environ. Exercise Physiol.* **56**, 1143–1150 (1984).
8. E. L. Hull, D. L. Conover, and T. H. Foster, "Carbogen-induced changes in rat mammary tumour oxygenation reported by near infrared spectroscopy," *Br. J. Cancer* **79**, 1709–1716 (1999).
9. C. M. Carpenter, R. Rakow-Penner, S. Jiang, B. W. Pogue, G. H. Glover, and K. D. Paulsen, "Monitoring of hemodynamic changes induced in the healthy breast through inspired gas stimuli with MR-guided diffuse optical imaging," *Med. Phys.* **37**, 1638–1646 (2010).
10. P. Vaupel, F. Kallinowski, and P. Okunieff, "Blood flow, oxygen and nutrient supply, and metabolic microenvironment of human tumors: a review," *Cancer Res.* **49**, 6449–6465 (1989).
11. N. J. Taylor, H. Baddeley, K. A. Goodchild, M. E. Powell, M. Thoumine, L. A. Culver, J. J. Stirling, M. I. Saunders, P. J. Hoskin, H. Phillips, A. R. Padhani, and J. R. Griffiths, "BOLD MRI of human tumor oxygenation during carbogen breathing," *J. Magn. Reson. Imaging* **14**, 156–163 (2001).